Supporting Information

Intrinsic and Stable Conjugation of Thiolated Mesoporous Silica Nanoparticles with Radioarsenic

Paul A. Ellison[†*◊], Feng Chen[‡§◊], Shreya Goel[‖], Todd E. Barnhart[†], Robert J Nickles[†], Onofre T. DeJesus[†], Weibo Cai[†‡‖ǂ]

[†]Department of Medical Physics, [‡]Department of Radiology, University of Wisconsin School of Medicine and Public Health, Madison, WI, USA, [§]Current affiliation: Memorial Sloan Kettering Cancer Center, New York, NY, USA, [‖]Materials Science Program and [ǂ]Carbone Cancer Center, University of Wisconsin, Madison, WI, USA

*Corresponding author: *paellison@wisc.edu*

[◊]P.A.E. and F.C. contributed equally to this work.

Equation S1: Quantification of thiol groups per nanoparticle

The number of thiol groups per nanoparticle was empirically calculated from its experimentally measured properties using the following equation:

$$N_{SH/np} = N_{AV} \cdot \frac{[SH]}{[m]} \cdot \frac{\frac{4}{3}\pi r^3}{\left(\frac{1}{\rho_{Si}} + V_p\right)},$$

where:

N_{AV} is Avagadro's number,

[m] is the nanoparticle mass concentration in g/mL as determined by mass measurement of lyophilized sample,

[SH] is the nanoparticle thiol concentration in nmol/mL as determined by Ellman's reagent quantification,

ρ_{Si} is the density of silica (assumed to be 2.2 g/mL),

V_p is the pore volume per gram of nanoparticles in cm^3/g as determined by Brunauer-Emmet-Teller (BET) measurement,

r is the nanoparticle radius in cm as determined by TEM measurement.

Table S1. Summary of decay properties, radionuclide production methods, and potential medical use of selected radioarsenic isotopes.

isotope	half-life (h)	decay properties[a]	production method	medical use	Most abundant γ emissions' energy (keV)	Most abundant β emissions' maximum energy (MeV)
^{71}As	65.30	28% β^+, 72% ec	Medical cyclotron	PET imaging	175 (82%) 1095 (4.1%)	0.82 (28%, β^+)
^{72}As	26.0	88% β^+, 12% ec	Medical cyclotron, ^{72}As/^{72}Se generator	PET imaging	834 (80%) 630 (7.9%)	2.5 (64%, β^+) 3.3 (16%, β^+)
^{74}As	426.5	29% β^+, 36% ec, 34% β^-	Medical cyclotron	PET imaging	596 (59%) 635 (15%)	0.94 (26%, β^+) 0.72 (15%, β^-)
^{76}As	25.867	100% β^-	Medical cyclotron	Radiotherapy	559 (45%) 657 (6.2%)	3.0 (51%, β^-) 2.4 (35%, β^-)
^{77}As	38.79	100% β^-	Medical cyclotron, neutron capture	Radiotherapy	239 (1.6%) 521 (0.56%)	0.68 (97%, β^-) 0.44 (1.6%, β^-)

[a] β^+: positron emission, ec: electron capture, β^-: electron emission.

Table S2. Quantification of PET results shown in Figures 6 and 7 for three ROIs of interest (liver, spleen, and bladder).

%ID/g (n = 3)		Free *As	*As-$dSiO_2$	*As-MSN(3nm pores)	*As-MSN(5nm pores)
0.5 – 1 h	**Liver**	7 ± 1	32 ± 3	34 ± 2	24 ± 1
	Spleen	n/a	11 ± 3	n/a	17 ± 5
	Bladder	35 ± 2	4.3 ± 0.2	18 ± 12	5 ± 2
3 – 6 h	**Liver**	1.1 ± 0.1	29 ± 2	34 ± 2	23 ± 2
	Spleen	n/a	10 ± 1	n/a	18 ± 5
	Bladder	45 ± 63	4 ± 4	23 ± 9	5 ± 4
~1 d	**Liver**	0.09 ± 0.02	27 ± 1	27 ± 4	23 ± 1
	Spleen	n/a	8 ± 2	n/a	24 ± 6
	Bladder	2 ± 1	5 ± 4	8 ± 6	3 ± 2
~3 d	**Liver**	n/a	26 ± 1	20 ± 3	27 ± 2
	Spleen	n/a	10 ± 2	n/a	36 ± 8
	Bladder	n/a	4.0 ± 0.9	4 ± 1	2.8 ± 0.6
~5 d	**Liver**	n/a	23 ± 3	15 ± 1	30 ± 1
	Spleen	n/a	11 ± 3	n/a	38 ± 6
	Bladder	n/a	5 ± 2	2 ± 1	2.4 ± 0.6
~7 d	**Liver**	n/a	21 ± 6	14 ± 2	30 ± 4
	Spleen	n/a	11 ± 2	n/a	45 ± 10
	Bladder	n/a	3.8 ± 0.5	1.4 ± 0.8	1.4 ± 0.9

Table S3. Quantification of 7 day post-injection *ex vivo* biodistribution shown in Figures 7d.

%ID/g (n = 3)	*As-dSiO$_2$	*As-MSN (3nm pores)	*As-MSN (5nm pores)
Blood	0.0 ± 0.2	0.02 ± 0.01	0.1 ± 0.2
Skin	0.17 ± 0.02	1.0 ± 0.4	0.3 ± 0.1
Muscle	0.03 ± 0.02	0.016 ± 0.004	0.1 ± 0.1
Bone	0.3 ± 0.2	0.21 ± 0.04	1.2 ± 0.5
Heart	0.07 ± 0.02	0.03 ± 0.01	0.3 ± 0.3
Lung	1.6 ± 1.4	0.25 ± 0.07	3 ± 2
Liver	15 ± 2	25 ± 3	35 ± 10
Kidney	0.089 ± 0.005	0.06 ± 0.02	0.08 ± 0.02
Spleen	28 ± 6	18 ± 9	110 ± 70
Pancreas	0.04 ± 0.02	0.03 ± 0.01	0.2 ± 0.2
Stomach	0.20 ± 0.03	0.05 ± 0.04	0.1 ± 0.1
Intestine	0.18 ± 0.05	0.06 ± 0.06	0.08 ± 0.03
Tail	n/a	0.2 ± 0.1	4 ± 5
Brain	0.006 ± 0.001	0.03 ± 0.03	0.1 ± 0.1

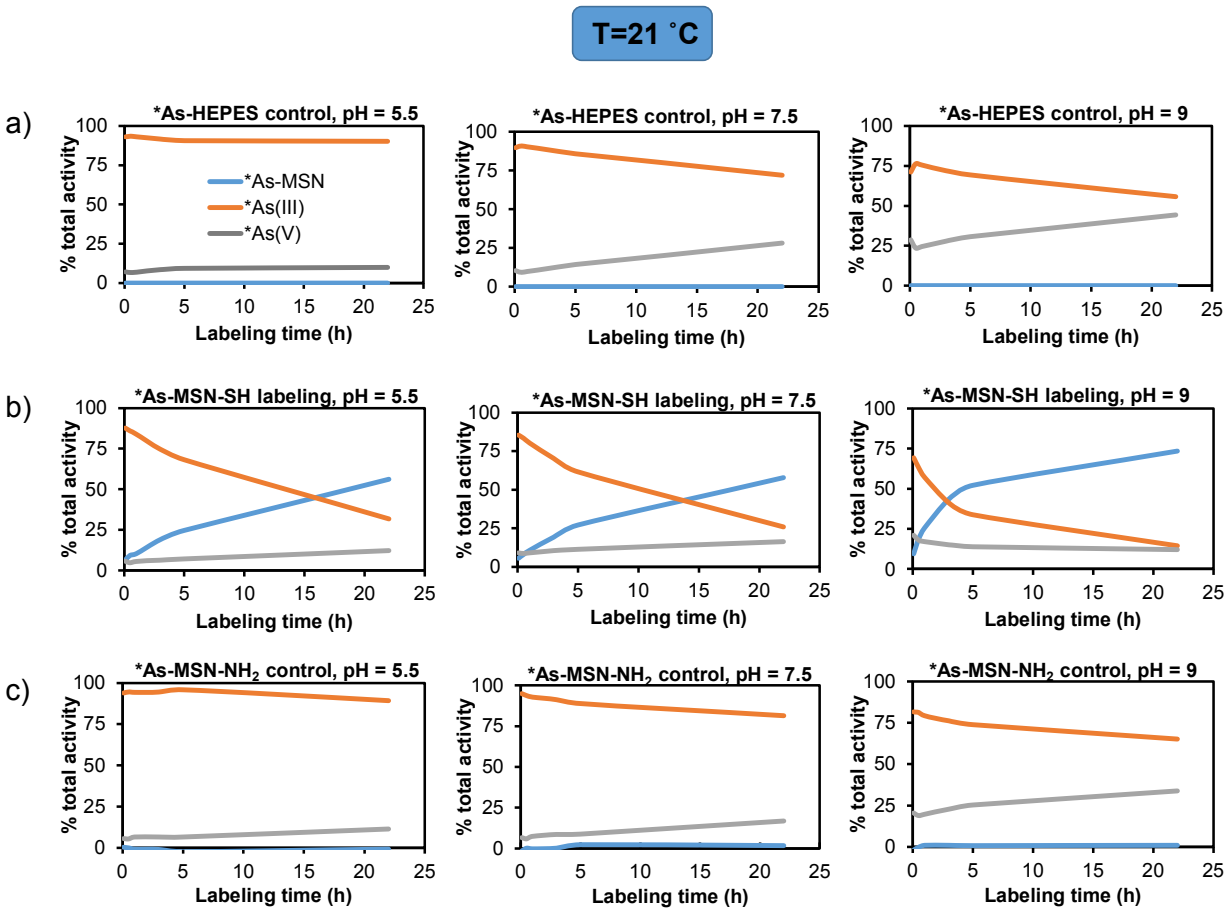

Figure S1. Results of radio-TLC analysis of *As(III) labeling at 21 ˚C and pH 5.5 (left), 7.5 (middle), or 9.5 (right) of (a) control vial containing only labeling medium (0.1 M HEPES, 0.5 M HA, 25 mM EDTA), (b) 600 nmol (-SH)/mL MSN(3nm pores)-SH in 0.1 M HEPES, 70 mM HA, 3 mM EDTA solutions, and (c) 520 nmol(-NH_2)/mL MSN(3nm)-NH_2 in 0.1 M HEPES, 70 mM HA, 3 mM EDTA solutions. Radio-TLC quantification methods resulted in high uncertainty in solutions containing nearly 0% *As(III) and nearly 100% *As(V).

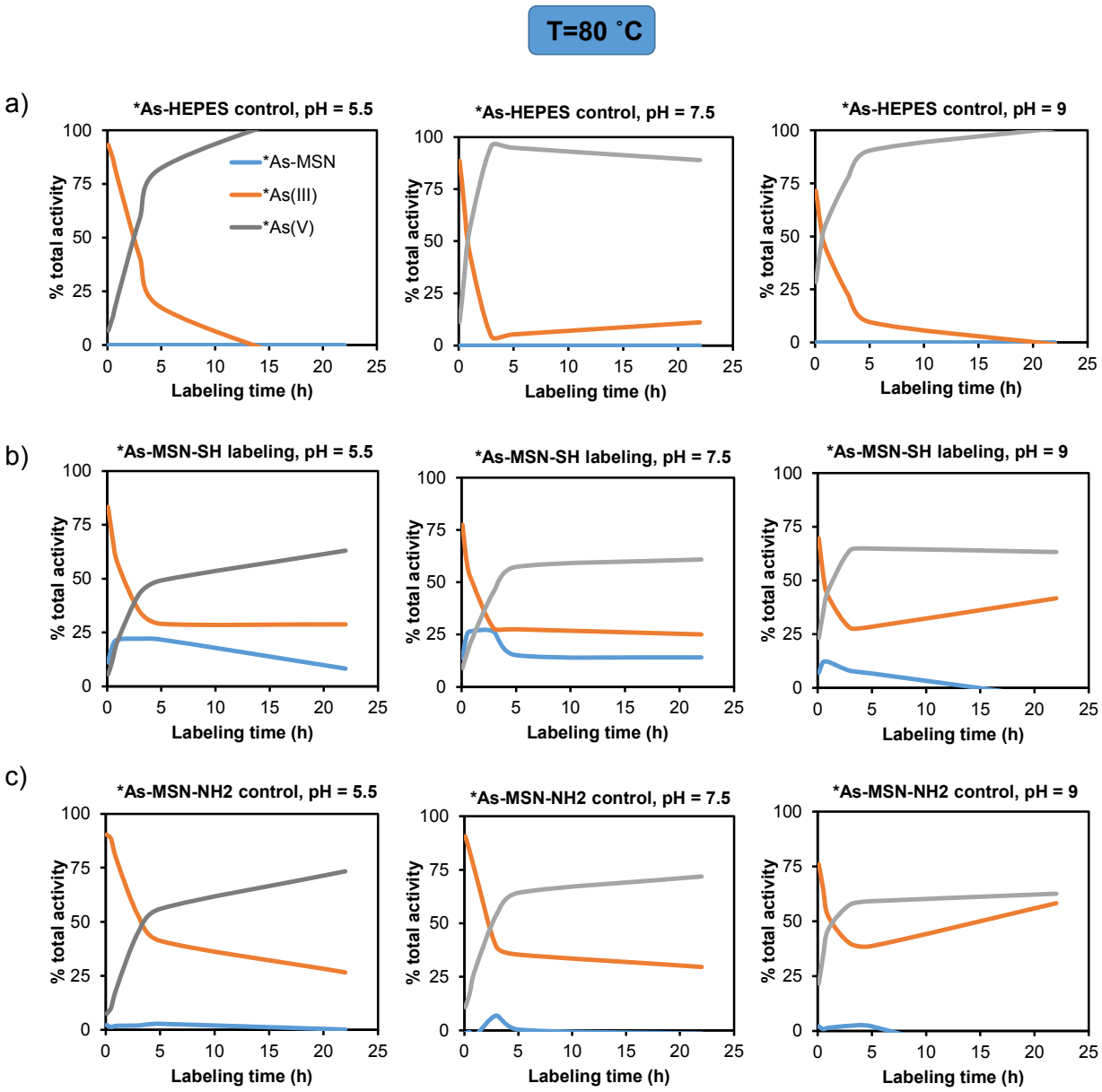

Figure S2. Results of radio-TLC analysis of *As(III) labeling at 80 ˚C and pH 5.5 (left), 7.5 (middle), or 9.5 (right) of (a) control vial containing only labeling medium (0.1 M HEPES, 0.5 M HA, 25 mM EDTA), (b) 600 nmol (-SH)/mL MSN(3nm pores)-SH 0.1 M HEPES, 70 mM HA, 3 mM EDTA solutions, and (c) 520 nmol(-NH_2)/mL MSN(3nm)-NH_2 in 0.1 M HEPES, 70 mM HA, 3 mM EDTA solutions. Radio-TLC quantification methods resulted in high uncertainty in solutions containing nearly 0% *As(III) and nearly 100% *As(V).

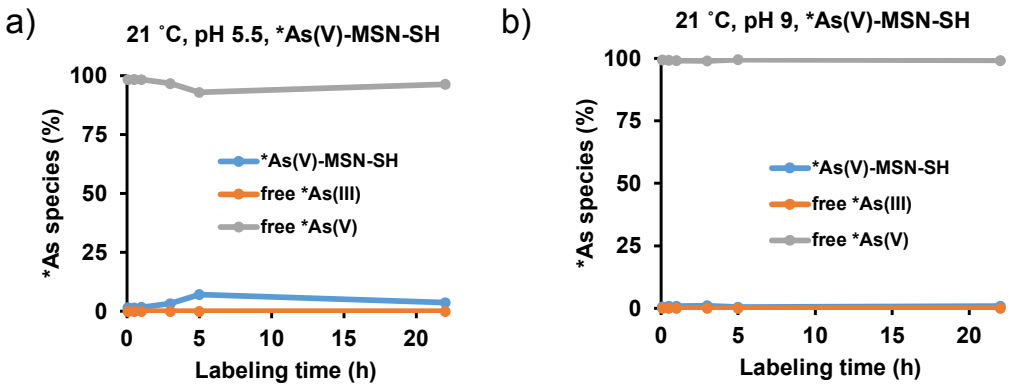

Figure S3. Results of radio-TLC analysis of *As(V) labeling at 21 ˚C of 490 nmol(-SH)/mL MSN(3nm)-SH in 0.1 M HEPES, 0.14 M HA, 7 mM EDTA solutions at (a) pH 5.5 and (b) pH 9. Radio-TLC quantification methods resulted in high uncertainty in solutions containing nearly 0% *As(III) or *As-MSN and nearly 100% *As(V).